

Protocol-dependent shear modulus of amorphous solids

Daiyu Nakayama,^{1,2} Hajime Yoshino,^{1,2} and Francesco Zamponi³

¹*Cybermedia Center, Osaka University, Toyonaka, Osaka 560-0043, Japan*

²*Graduate School of Science, Osaka University, Toyonaka, Osaka 560-0043, Japan*

³*Laboratoire de Physique Théorique, ENS & PSL University, UPMC & Sorbonne Universités, UMR 8549 CNRS, 75005 Paris, France*

We investigate the linear elastic response of amorphous solids to a shear strain at zero temperature. We find that the response is characterized by at least two distinct shear moduli. The first one, μ_{ZFC} , is associated with the linear response of a single energy minimum. The second, μ_{FC} , is related to sampling, through plastic events, an ensemble of distinct energy minima. We provide examples of protocols that allow one to measure both shear moduli. In agreement with a theoretical prediction based on the exact solution in infinite spatial dimensions, the ratio $\mu_{\text{FC}}/\mu_{\text{ZFC}}$ is found to vanish proportionally to the square root of pressure at the jamming transition. Our results establish that amorphous solids are characterized by a rugged energy landscape, which has a deep impact on their elastic response, as suggested by the infinite-dimensional solution.

I. INTRODUCTION

Most solid state textbooks are almost entirely devoted to crystals [1]. The reason is obvious: while the theory of crystals is fully developed, the theory of amorphous solids (glasses, foams, granulars, etc.) is still very incomplete [2, 3]. Crystals can be understood as perfect periodic lattices, around which particles perform small vibrations. This allows one to construct a low-temperature harmonic expansion, and obtain all thermodynamic properties in terms of harmonic excitations, i.e. phonons. Moreover, crystal flow (or plasticity) and melting is mediated by defects (mostly dislocations) that are also quite well understood [1].

The situation is very different for glasses, which display all kind of anomalies with respect to crystals: they show an enhanced low-frequency density of states (the so-called Boson Peak) [4], leading to anomalous behavior of specific heat and thermal conductivity [5]. Crucially for our study, they show irreversible “plastic” response to arbitrarily small perturbations [6–10]: during plastic events, some part of the system relaxes irreversibly to a new low-energy state by crossing some low-energy barrier [11–15].

These observations suggest the following picture: crystals can be thought as isolated minima of the potential energy, around which a well-defined harmonic expansion can be performed, and that are separated from other minima by high enough energy barriers [1]. On the contrary, glasses are “fragile” minima of the potential energy function: they are characterized by many soft modes [16], the harmonic expansion thus works only at extremely low temperatures [17–19], and very low-energy barriers separate each glassy minimum from many other neighboring, and equivalent, glassy minima [11, 20, 21]. In this picture, it is natural that even a very small perturbation destabilizes a glassy minimum and brings the system over a barrier to relax, irreversibly, to another minimum [11, 14, 21].

The exact mathematical solution of the problem in the

abstract limit of an infinite-dimensional space can be the source of inspiration about some physical properties of the solid in three dimensions [22, 23]. In particular, it suggests that the organisation of the energy minima is hierarchical [21]: glassy minima are organised in clusters, or “basins”, themselves organised in larger basins, and so on, as it is well-known to happen in mean field spin glasses [24, 25]. In such a situation, the response of the glass to an external perturbation depends on how much of the energy landscape can be explored [24–27]. Consider elastic response. If only a given energy minimum is

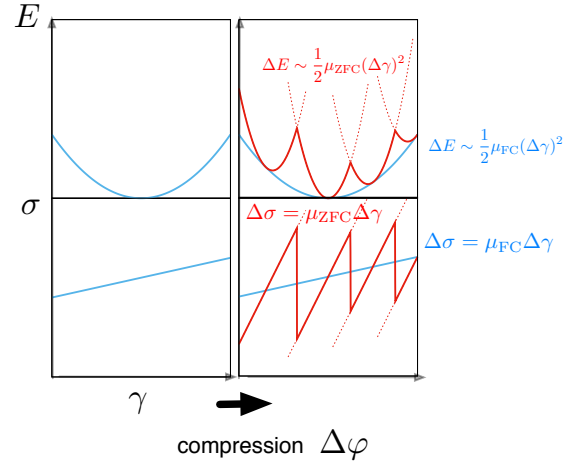


FIG. 1. Oversimplified sketch of an energy landscape with two distinct shear moduli. *Top*: elastic energy E versus shear strain γ . *Bottom*: same illustration using stress $\sigma = dE/d\gamma$ as a function of strain. Within a single energy minimum (left column), the energy increase behaves elastically $\Delta E \propto (\Delta\gamma)^2$ for a small enough increment of the shear strain $\Delta\gamma$. When the energy landscape becomes bifurcated (right column), energy minima (red line) are organised in basins (blue line). Each of the dotted line represents a region where a minimum is locally stable. If the system can sample the basin, a lower shear modulus μ_{FC} is observed in the $\gamma \rightarrow 0$ regime, corresponding to the envelope of the individual basins. The softening is due to inter-basin transitions.

explored, the system responds linearly with certain elastic coefficients. If a larger cluster of minima can be explored, the response is still linear, but elastic coefficients are different (see Fig. 1 for an illustration). Precise computations can be performed in the infinite-dimensional limit [27, 28].

In this paper, inspired by this idea, we explore the elastic response of the simplest amorphous solid, a zero-temperature jammed assembly of soft spheres at pressure P , to the simplest perturbation, shear strain. We focus on the vicinity of the jamming transition, which happens at the density where $P = 0$ for the first time upon decompression [29]. By analogy with spin glasses [24], we use two distinct measurement protocols to determine the linear shear modulus: in the “zero-field compression” (ZFC) protocol, one first reaches the target pressure and then applies the shear strain; in the “field compression” (FC) one first applies the shear strain, and then compresses to target pressure P . The terminology comes from spin glasses where the strain is replaced by a magnetic field [24].

We obtain three main results. *(i)* We show that in the ZFC protocol, the response is elastic with a shear modulus μ_{ZFC} that characterizes a single glassy minimum. In the FC protocol the response turns out to be still elastic but with a distinct shear modulus $\mu_{\text{FC}} < \mu_{\text{ZFC}}$ due to plastic events or inter-valley transitions, similarly to what happens with magnetic susceptibility in spin glasses [24, 25, 30, 31]. This result suggests a non-trivial organisation of glassy minima (but does not prove that it is hierarchical as in the infinite-dimensional solution). *(ii)* Infinite-dimensional calculations predict that in the limit in which the solid unjams, and $P \rightarrow 0$, the hierarchical organisation of basins becomes fractal [21]; in this limit, it is predicted that $\mu_{\text{ZFC}} \propto P^{1/2}$ while $\mu_{\text{FC}} \propto P$, thus $\mu_{\text{FC}} \ll \mu_{\text{ZFC}}$ resulting in a sharp separation of the two shear moduli [27]. Our numerical data agree with the theoretical prediction. *(iii)* We find that μ_{FC} decreases with increasing system size, suggesting that $\mu_{\text{FC}} = 0$ in the thermodynamic limit. This finding is not consistent with the most naive expectation based on the infinite-dimensional solution, and could be due to several aspects of our numerical simulation protocol, as we discuss below.

II. METHODS

A. Details of the system

We study a 3-dimensional system of $N = 1000 - 4000$ particles interacting via a soft repulsive contact pair potential

$$U = \sum_{i < j} \phi_{ij}(r_{ij}) , \quad (1)$$

where $r_{ij} = |\mathbf{r}_{ij}| = |\mathbf{r}_i - \mathbf{r}_j|$ is the distance between particles i and j , and $\phi_{ij}(r) = \epsilon(1 - r/D_{ij})^2$ for $r < D_{ij}$ and zero otherwise. Here $D_{ij} = (D_i + D_j)/2$ where D_i is the

diameter of the i -th particle. To avoid crystallization, we consider a binary mixture of $N/2$ particles with diameter D_1 and $N/2$ particles with diameter D_2 with the ratio $D_2/D_1 = 1.4$. This is a standard choice in studies of jamming [29, 32].

In thermal equilibrium, the control parameters are reduced temperature $\hat{T} = k_B T / \epsilon$ and volume fraction $\varphi = (\pi/12)(D_1^3 + D_2^3)\rho$, where $\rho = N/V$ is the number density and V is the volume of the system. Note that inflating the particles by increasing the diameters $D_{1,2}$ is completely equivalent to reducing the volume V : both operations amount to an increase of φ at constant \hat{T} , i.e. a compression. The main observables we consider are pressure, which is the response of the system to a change in its volume:

$$P = -\frac{1}{3V} \sum_{i < j} \mathbf{r}_{ij} \cdot \nabla \phi_{ij}(r_{ij}) , \quad (2)$$

and shear-stress, which is the response to a volume-preserving change of boundary conditions corresponding to a shear-strain:

$$\sigma = \frac{1}{V} \sum_{i < j} x_{ij} z_{ij} (\phi'_{ij}(r)/r)_{r=r_{ij}} , \quad (3)$$

where x_{ij}, z_{ij} are x and z components of the vector \mathbf{r}_{ij} . Eqs. (2) and (3) provide the microscopic expressions of pressure and shear-stress for a given particle configuration; these expressions must be averaged over an appropriate ensemble of configurations, as described below. Throughout the paper, ϵ and D_1 are used as units of energy and length.

B. Preparation of the samples

Each of our $\mathcal{N}_s = O(10^4)$ independent “samples” is obtained as follows. We start by a random configuration at $\varphi_{\text{init}} = 0.64$ and we run molecular dynamics (MD) simulation at $\hat{T} = 10^{-5}$ for $30\tau_{\text{col}}$, where τ_{col} is the typical collision time. This is done in order to stabilize the system against small thermal fluctuations within the initial energy basin selected by the random configuration, similarly to [18]. However, note that $\hat{T} = 10^{-5}$ is such a low temperature that no barrier crossing to other glassy basins can occur, so our system effectively remains trapped into a random energy basin, selected by the initial random configuration [18, 32]. This will be a crucial observation for the following discussion.

Next, we bring the system to $\hat{T} = 0$ by energy minimization using the conjugated gradient (CG) method [33], i.e. we reach an energy minimum close to the thermally stabilized configurations. We obtain in this way our initial configurations at $\hat{T} = 0$ and φ_{init} , and from now on we always work at zero temperature. Note that $\varphi_{\text{init}} = 0.64$ is lower than the jamming density $\varphi_j \approx 0.6466$ [18, 29] and thus the initial configurations are unjammed, i.e. they have zero pressure.

C. Measurement protocols

To each sample we then apply two different protocols to measure the shear modulus, inspired by the ones used in spin glasses [25, 30, 31]. They consist in compressing the samples in presence or in absence of a shear strain.

Before describing the protocols, we specify that (de)compression is done in small steps, during which the system is subjected to (i) affine deformation (multiplying by a common factor all particles' diameters in such a way that φ changes by an amount $d\varphi = 5.0 \times 10^{-3}$) followed by (ii) energy minimization via CG. Shear strain γ is also applied in two steps by (i) affine deformation, where $x_i \rightarrow x_i + \gamma z_i$ for all particles (boundary condition into the z direction are also shifted by the Lees-Edwards scheme [34]), followed by (ii) energy minimization via CG.

In the Field Compression (FC) protocol, the system is first subjected to a shear γ at φ_{init} . Then it is adiabatically compressed (AC) in small steps (affine deformation + CG) up to $\varphi_f = 0.66$ corresponding to a pressure $P_f \simeq 0.014$. The remanent shear stress $\sigma(P, \gamma)$ is measured at fixed values of the pressure $P \in [0, P_f]$, and from it we deduce the FC shear modulus $\mu_{\text{FC}}(P, \gamma) = \sigma(P, \gamma)/\gamma$. Next, the system is adiabatically decompressed (AD) back to φ_{init} and the same measurements are performed along the way. In the Zero-Field Compression (ZFC), the system is AC up to the same P_f and then AD in small steps in absence of any shear. The stress and pressure are measured after each step of the compression and decompression. To measure the stress, in the ZFC case we take the current configuration and apply to it a small strain γ , and measure $\mu_{\text{ZFC}}(P, \gamma) = \sigma(P, \gamma)/\gamma$; the sheared configuration is then discarded.

In both cases, the averages over different samples are done at constant pressure and not at constant φ : in fact, due to finite-size effects, the jamming point φ_j where pressure vanishes depends on the sample [29]. If we want to study the scaling for $P \rightarrow 0$ it is better to average at constant pressure than at constant density. In practice, averaging over the samples with a given pressure P is done by collecting data in the range $[P, P + dP]$ choosing some dP . We examined dP in the range $O(10^{-5}) - O(10^{-3})$ and found that its precise choice is irrelevant: here we choose it such that we have a good number of samples in each pressure bin.

In the ZFC process we also measure the shear modulus directly at $\gamma = 0$ via the “fluctuation formula” [8]:

$$\mu_{\text{ZFC}}(P, \gamma = 0) = b - \frac{1}{V} \sum_{i=1}^N \Xi_i \cdot (\mathcal{H}^{-1} \Xi)_i. \quad (4)$$

Here b is the Born term (affine part of μ) defined as

$$b = \frac{1}{V} \sum_{i < j} \left(z_{ij} \frac{\partial}{\partial x_{ij}} \right)^2 \phi(r_{ij}) \quad (5)$$

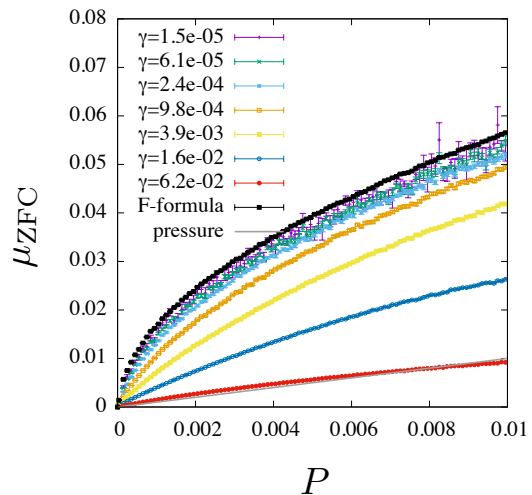


FIG. 2. ZFC shear modulus, for which AC and AD give indistinguishable results. $N = 1000$ is used for the analysis of μ_{ZFC} . Data with various values of the strain $\gamma = 2^{-9}, 2^{-8}, \dots, 2^{-3}$ are shown. $dP = 10^{-4}$ is used for binning. The number of samples for each bin is $O(10^4)$. “F-formula” indicates data obtained via fluctuation formula.

while the second term is the non-affine correction, defined by the Hessian matrix

$$\mathcal{H}_{ij}^{\mu\nu} = \delta_{\mu\nu} \delta_{ij} \sum_{k=1}^N \phi^{\mu\mu}(r_{ik}) - \phi^{\mu\nu}(r_{ij}), \quad \phi^{\mu\nu}(r_{ij}) \equiv \frac{\partial^2 \phi(r_{ij})}{\partial x_i^\mu \partial x_j^\nu}$$

where $\mu, \nu = x, y, z$, and $\Xi_i = \nabla_i \sigma$. Note that this zero-temperature formula assumes purely harmonic response excluding any plasticity. Its finite-temperature version, on the contrary, can take into account all kinds of thermal excitations including plastic ones [26]. Note also that, unfortunately, there is no analog of the fluctuation formula for the FC measurement: in fact, while the linear ZFC shear modulus is a property of a single configuration and can thus be written as in Eq. (4), in the FC case the linear shear modulus is a property of the whole basin and for that reason a fluctuation formula necessarily involves an averaging over different minima in a basin with weights that are difficult to determine [27].

III. RESULTS

A. Zero-field compression

We first discuss results obtained with the ZFC protocol. We note that ZFC is the standard protocol that has been used in a number of previous studies [29, 35], so we can directly compare our data with previous work.

In Fig. 2 we report results for μ_{ZFC} obtained at constant pressure P and for several values of shear strain γ . We observe that at large γ there is a strong non-linear contribution and $\mu_{\text{ZFC}} \sim P$, but upon lowering γ the

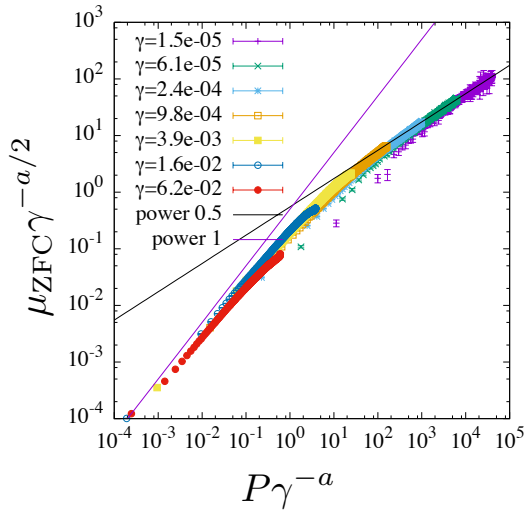


FIG. 3. ZFC shear modulus, scaled according to Eq. (6) with $a = 4/3$. Here $dP = 2.5 \times 10^{-5}$ and $O(10^3)$ samples are in each bin.

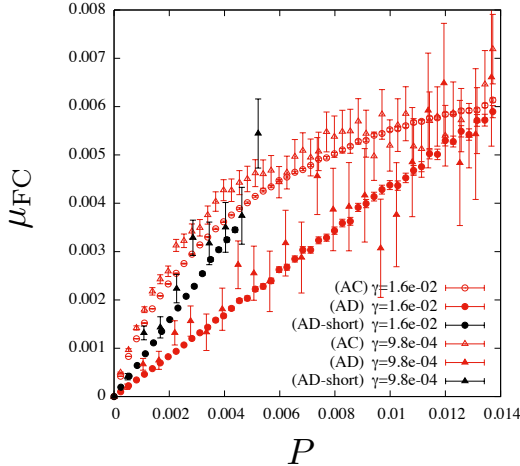


FIG. 4. FC shear modulus measured under compression and decompression. Here data sets of $N = 1000$ with $\gamma = 2^{-6} \simeq 1.6 \times 10^{-2}$ and $\gamma = 2^{-8} \simeq 9.8 \times 10^{-4}$. For the decompression, data obtained returning from $\varphi_f = 0.66$ ($P_f \simeq 0.005$) (AD-short) and $\varphi_f = 0.68$ ($P_f \simeq 0.014$) (AD) are shown. $dP = 10^{-4} - 5 \times 10^{-3}$ and the number of samples for each bin is $O(10^5)$ for AC, $O(10^4)$ for AD.

linear response regime emerges, because the curves converge towards the result obtained using the fluctuation formula. This result confirms that μ_{ZFC} is indeed a property of a single energy minimum, as it can be measured with the fluctuation formula while the system sits in the minimum without applying any perturbation.

Also, μ_{ZFC} is found, as in previous work [29], to scale proportionally to $P^{1/2}$ when $P \rightarrow 0$. In order to have a clean demonstration of this behavior, we collapse all curves at finite γ using the form proposed in [36] in the framework of a proposed scaling theory of the jamming

transition :

$$\mu_{\text{ZFC}}(P, \gamma) = \gamma^{a/2} F(P/\gamma^a). \quad (6)$$

Here, $F(x \rightarrow \infty) \sim x^{1/2}$, while $F(x \rightarrow 0) \sim x$. This implies $\mu_{\text{ZFC}}(P, \gamma \rightarrow 0) \sim P^{1/2}$, while $\mu_{\text{ZFC}}(P \rightarrow 0, \gamma > 0) \sim P\gamma^{-a/2}$. In Fig. 3 we report a very good data collapse using the value of $a = 4/3$ proposed in [36]. The very good coincidence with the prediction of [36] confirms the validity of the scaling theory of jamming proposed there. Furthermore, this result confirms the scaling of $\mu_{\text{ZFC}}(P, \gamma = 0) \sim P^{1/2}$ [29] and extends it to the non-linear regime [36–38]. Although finite size effects may appear at lower values of the pressure approaching the unjamming point, we checked that there is no signature of finite size effects within the range of pressure we studied down to $P = O(10^{-4})$ and system sizes $N = 500 - 2000$. Note *en passant* that, although this is not the main focus of this paper, the result in Eq. (6), proposed in [36], to the best of our knowledge has not been tested numerically before, and therefore it is an original result of this work.

B. Field compression

We now turn to the discussion of the FC shear modulus, which is reported in Fig. 4. First, we note that while for μ_{ZFC} adiabatic compression (AC) and decompression (AD) give identical results, this is not the case for μ_{FC} . During AC, μ_{FC} grows linearly at small P and then saturates at larger P ; it remains larger during AC than during AD. By comparing results for two different final values of pressure P_f (see Fig. 4), we note that the AD curves connects perfectly linearly the final value of stress just before starting the decompression and 0, which seems to be a general feature of the AD curves. We also found that the AD curve is reversible, i. e. the stress follows exactly the AD curve under re-compression.

Moreover, while μ_{ZFC} deviates from the linear regime for quite small γ ($\gamma \sim 10^{-4}$, see Fig. 2), here we observe that μ_{FC} is almost independent of γ in a regime of shear strain that is larger by two orders of magnitude, $\gamma \lesssim 10^{-2}$. We conclude that $\mu_{\text{FC}}(P)$ is measured in the linear response regime, and is proportional to P at low pressure both in AC and AD protocols (although with different coefficients).

Having established the existence of a linear regime for both FC and ZFC shear moduli, in Fig. 5 we compare the two. We find that at all pressures, $\mu_{\text{FC}} < \mu_{\text{ZFC}}$, with $\mu_{\text{FC}} \sim P \ll \mu_{\text{ZFC}} \sim P^{1/2}$ in the jamming limit.

C. Comparison between glassy and crystalline solids

In Fig. 5, we compare the results for the amorphous solids with the results for the FCC crystal, whose close packing density is $\varphi_c \simeq 0.72$. The ZFC shear modulus

of the FCC system is obtained using the fluctuation formula. We found that the non-affine correction term is absent in the FCC case. On the other hand the FC shear modulus of the FCC system is obtained performing precisely the same analysis as we did for the glassy system. As expected, we find no difference between the FC and ZFC shear moduli in the crystalline system.

D. Finite size effects

In Fig. 6 and Fig. 7 we study the system size dependence of μ_{FC} . We observe that μ_{FC} decreases upon increasing N and that $N^{\alpha(\gamma)}\mu_{\text{FC}}$ is approximately constant with a shear strain-dependent exponent $\alpha(\gamma)$, which suggests that $\mu_{\text{FC}} = 0$ in the thermodynamic limit for our samples. However, we only obtained data on three sizes and the proposed $N^{-\alpha}$ behavior works with an exponent α that is not so big. There might be still the opportunity that the infinite size limit of μ_{FC} is compatible also with a finite value, or that we are in a pre-asymptotic limit for the finite size scaling. Finally, recall that we do not observe significant finite size effects for μ_{ZFC} .

IV. COMPARISON WITH MEAN FIELD THEORY

As discussed in the introduction, the design of our numerical simulation has been inspired by the analytical solution of the infinite dimensional problem, which provides a mean field theory for the problem and establishes an analogy with mean field spin glasses. Although our work is not meant to be a precise test of the theory, it is still useful to compare our findings to what is expected on the basis of the mean field picture.

First of all, we have found that $\mu_{\text{FC}} < \mu_{\text{ZFC}}$, as suggested by the theory. Moreover, upon approaching jamming, $\mu_{\text{FC}} \sim P \ll \mu_{\text{ZFC}} \sim P^{1/2}$, which is also consistent with the theoretical expectation. The fact that μ_{FC} is strongly dependent on the protocol (e.g. it is different for AC and AD protocols, as shown in Fig. 4) is also expected from the theory: because μ_{FC} results from an averaging over minima within a basin, its value depends on the way this minima are sampled out of equilibrium [27]. All these results are thus qualitatively consistent with the theoretical expectation.

There is one result, however, that deserves a more detailed discussion: the system size dependence of μ_{FC} . Mean field theory predicts that glassy states prepared by slow annealing from the liquid should fall within hierarchically-organised basins [39, 40], having a FC shear modulus that remains finite in the thermodynamic limit. Another theoretical approach is to put a uniform weight (*à la Edwards*) over all possible glassy states: this leads to similar results [21]. Our preparation protocol instead starts from totally random *initial* configurations, which are instantaneously cooled to very low tempera-

ture, and then to zero temperature (see Section II B): this is very different from preparing a glass by slow annealing or by giving the same weight to all possible glassy states [22, 41–43]. This is a possible reason that explains why μ_{FC} is observed to vanish for $N \rightarrow \infty$: our samples have been prepared very far from equilibrium and therefore do not belong to fully stabilized glassy metabasins. How to compute properties of these states within mean field theory remains an open question: it could be possible using dynamical methods such as the ones introduced in [44]. It would thus be interesting to repeat this study using fully stabilised glasses for which theoretical predictions have been successfully tested [40]: but this is much more computationally demanding and we leave it for the future. Another possibility that we cannot exclude is that specific finite-dimensional effects lead to the vanishing of μ_{FC} in all glassy states: to test this idea, one should repeat the present study in different spatial dimensions to see if a systematic trend with dimension emerges [45].

V. DISCUSSION

In this paper we have shown that the shear modulus of a simple amorphous solid at zero temperature is protocol dependent: there are at least two distinct shear moduli in the linear response regime. The FC protocol, in which strain is applied before compression, leads to softer glasses than the ZFC protocol, in which strain is applied after compression. The infinite-dimensional solution of the problem provides a natural interpretation of this result [27, 28]. In the ZFC protocol the system is first prepared in a minimum of the energy, then strain is applied. In this way one probes the response of a single energy minimum. We confirm this by showing that μ_{ZFC} can be equivalently obtained by the fluctuation formula, i.e. without applying strain but using linear response in the vicinity of a single minimum. In the FC instead, the strain is applied before compression, and during compression the system is allowed to explore, through plastic events, some part of a larger “basin” composed by several energy minima. In this way more stress can be relaxed, leading to a softer response, $\mu_{\text{FC}} < \mu_{\text{ZFC}}$. Note that while plastic events themselves are non-linear processes from the microscopic point of view, they give rise to a “renormalized”, softer linear response at the macroscopic level. This result suggests the presence of at least two “structures” in the energy landscape: minima, and basins of minima (Fig. 1).

We also find that upon approaching the jamming point where pressure vanishes, the ratio $\mu_{\text{FC}}/\mu_{\text{ZFC}} \propto P^{1/2}$ vanishes. This result is consistent with the theoretical prediction obtained in infinite spatial dimensions where the structure of minima inside clusters is hierarchical and fractal [21, 27]. It thus hints at a very complex landscape characterized by many nested “structures”.

Finally, we find that for the numerically investigated samples, $\mu_{\text{FC}} \rightarrow 0$ in the thermodynamic limit, contrary

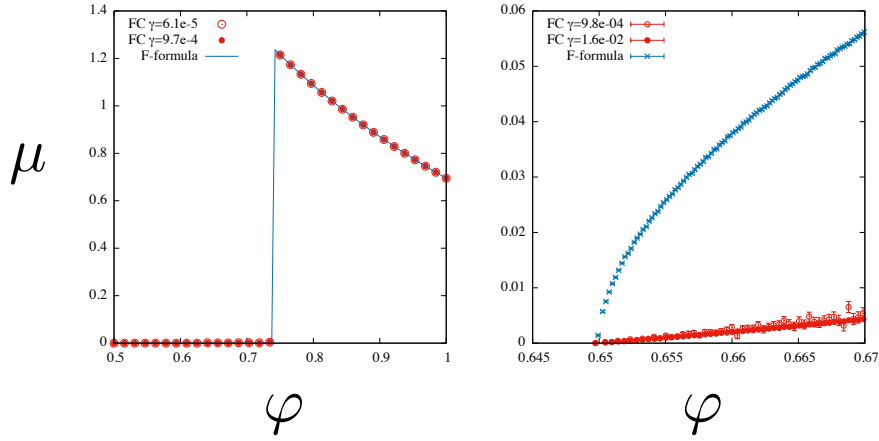


FIG. 5. Comparison of the ZFC (blue) and FC (red) shear modulus of the FCC crystal (left) and the glassy system (right). For the crystal and glassy systems $N = 864$ and $N = 1000$ are used respectively, and we use the AD protocol for the FC shear modulus of the glass. In both cases, the fluctuation formula is used to obtain the ZFC shear-modulus. For the glassy system, binning is done by $dP = 5.0 \times 10^{-3}$ for FC and $dP = 10^{-4}$ for ZFC by which the number of samples for each bin becomes $O(10^4)$. $\mu_{FC} < \mu_{ZFC}$ for all pressures in the glassy system.

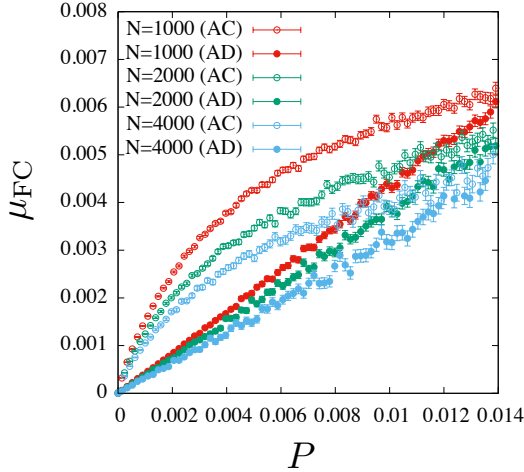


FIG. 6. Finite size effects of the FC shear modulus. $\gamma = 2^{-6} \simeq 1.6 \times 10^{-2}$, $dP = 10^{-4}$ and the number of samples for each bin is $O(10^4)$.

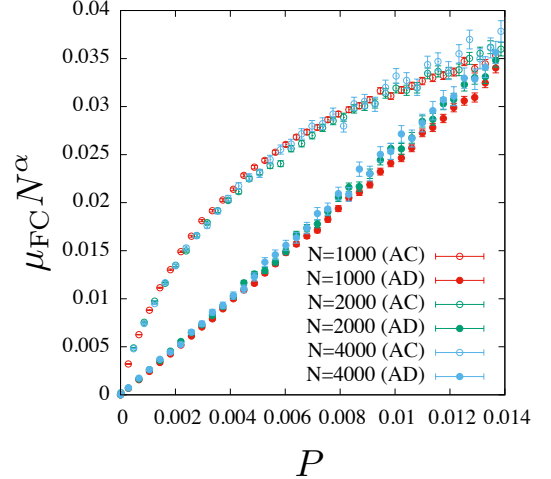


FIG. 7. Finite size scaling of the FC shear modulus. Here the data shown in Fig. 6 are used. The exponent is $\alpha = 0.25$.

to what the theory predicts for fully stabilized glassy basins. We tentatively attribute the discrepancy to the fact that theory focuses on fully stabilized glasses, while in the numerical simulation we used glasses prepared from totally random configurations, see the discussion in Section IV.

Our results are related to other works and can be extended in several directions. Explorations of plasticity in amorphous solids have been reported in many studies [6–10], where the instability of energy minima under strain have been characterised in terms of soft energy modes [12–15]. In particular it has been suggested that plastic events happen for values of strain that vanish when $N \rightarrow \infty$ as power laws, $\delta\gamma \sim N^{-\beta}$ [12, 14, 15, 17], which suggests a non-trivial linear response even in the

vicinity of a single minimum. It would be interesting to check whether this is consistent with our results and with theoretical predictions. It is interesting to note that the cartoon in Fig. 1 immediately suggests that if one defines \bullet as the average over states, then $d\bar{\sigma}/d\gamma \neq \bar{d\sigma}/d\gamma$, consistently with the results of [46]. Furthermore, our results imply that there is dissipation even at zero frequency, hence the dissipative part of the frequency-dependent shear modulus does not go to zero at low frequency, as in solid friction. This is one of the signatures of soft glassy rheology [47], and is typical of energy landscapes with cusps like the one studied in [48]. Another interesting issue is that of non-linear responses, which are suggested to be strongly anomalous both by theory [49] and numerical simulations [12, 37, 46], in close relation with the complexity of the landscape suggested by our results. Finally,

a crucial question is whether, upon adding temperature, the difference $\mu_{FC} < \mu_{ZFC}$ persists until the glass melts, or there is a well defined temperature (a Gardner temperature) above which the glass becomes a normal solid with $\mu_{FC} = \mu_{ZFC}$ [21, 40].

ACKNOWLEDGMENTS

We warmly thank Jean-Philippe Bouchaud for bringing this problem to our attention and for many inspiring

discussions, and we thank two anonymous referees for suggesting important improvements to a previous version of this manuscript. We also thank Giulio Biroli, Hisao Hayakawa, Andrea Liu, Michio Otsuki, Giorgio Parisi, Corrado Rainone, Pierfrancesco Urbani and Yuliang Jin for many useful discussions. This work was supported by KAKENHI (No. 25103005 “Fluctuation & Structure” and No. 50335337) from MEXT, Japan, by JPS Core-to-Core Program “Non-equilibrium dynamics of soft matter and informations”. The Computations were performed using Research Center for Computational Science, Okazaki, Japan.

-
- [1] N. W. Ashcroft and N. D. Mermin, *Solid State Physics* (Thomson Learning, 1976).
 - [2] L. Berthier and G. Biroli, *Rev. Mod. Phys.* **83**, 587 (2011).
 - [3] A. Cavagna, *Physics Reports* **476**, 51 (2009).
 - [4] V. K. Malinovsky and A. P. Sokolov, *Solid State Commun.* **57**, 757 (1986).
 - [5] W. A. Phillips, *Rep. Prog. Phys.* **50**, 1657 (1987).
 - [6] D. L. Malandro and D. J. Lacks, *The Journal of Chemical Physics* **110**, 4593 (1999).
 - [7] G. Combe and J.-N. Roux, *Physical Review Letters* **85**, 3628 (2000).
 - [8] C. Maloney and A. Lemaître, *Phys. Rev. Lett.* **93**, 195501 (2004).
 - [9] D. Rodney, A. Tanguy, and D. Vandembroucq, *Modelling and Simulation in Materials Science and Engineering* **19**, 083001 (2011).
 - [10] H. G. E. Hentschel, P. K. Jaiswal, I. Procaccia, and S. Sastry, *Phys. Rev. E* **92**, 062302 (2015).
 - [11] M. Goldstein, *The Journal of Chemical Physics* **51**, 3728 (1969).
 - [12] H. G. E. Hentschel, S. Karmakar, E. Lerner, and I. Procaccia, *Phys. Rev. E* **83**, 061101 (2011).
 - [13] C. Brito and M. Wyart, *J. Chem. Phys.* **131**, 024504 (2009).
 - [14] M. Wyart, *Physical Review Letters* **109**, 125502 (2012).
 - [15] M. Müller and M. Wyart, *Annu. Rev. Condens. Matter Phys.* **6**, 177 (2015).
 - [16] M. Wyart, S. Nagel, and T. Witten, *Europhysics Letters* **72**, 486 (2005).
 - [17] C. F. Schreck, T. Bertrand, C. S. O’Hern, and M. D. Shattuck, *Phys. Rev. Lett.* **107**, 078301 (2011).
 - [18] A. Ikeda, L. Berthier, and G. Biroli, *J. Chem. Phys.* **138**, 12A507 (2013).
 - [19] E. DeGiuli, E. Lerner, and M. Wyart, *The Journal of Chemical Physics* **142**, 164503 (2015).
 - [20] A. Heuer, *Journal of Physics: Condensed Matter* **20**, 373101 (2008).
 - [21] P. Charbonneau, J. Kurchan, G. Parisi, P. Urbani, and F. Zamponi, *Nature Communications* **5**, 3725 (2014).
 - [22] G. Parisi and F. Zamponi, *Rev. Mod. Phys.* **82**, 789 (2010).
 - [23] P. Charbonneau, J. Kurchan, G. Parisi, P. Urbani, and F. Zamponi, *arXiv:1605.03008* (2016).
 - [24] M. Mézard, G. Parisi, and M. A. Virasoro, *Spin glass theory and beyond* (World Scientific, Singapore, 1987).
 - [25] G. Parisi, *Proceedings of the National Academy of Sciences* **103**, 7948 (2006).
 - [26] H. Yoshino, *The Journal of Chemical Physics* **136**, 214108 (2012).
 - [27] H. Yoshino and F. Zamponi, *Physical Review E* **90**, 022302 (2014).
 - [28] C. Rainone and P. Urbani, *arXiv:1512.00341* (2015).
 - [29] C. S. O’Hern, L. E. Silbert, A. J. Liu, and S. R. Nagel, *Phys. Rev. E* **68**, 011306 (2003).
 - [30] K. Binder and A. P. Young, *Reviews of Modern Physics* **58**, 801 (1986).
 - [31] S. Nagata, P. Keesom, and H. Harrison, *Physical Review B* **19**, 1633 (1979).
 - [32] L. Berthier and T. A. Witten, *Phys. Rev. E* **80**, 021502 (2009).
 - [33] W. H. Press, *Numerical recipes 3rd edition: The art of scientific computing* (Cambridge university press, 2007).
 - [34] A. Lees and S. Edwards, *Journal of Physics C: Solid State Physics* **5**, 1921 (1972).
 - [35] A. Ikeda and L. Berthier, *Physical Review E* **92**, 012309 (2015).
 - [36] C. P. Goodrich, A. J. Liu, and J. P. Sethna, *arXiv:1510.03469* (2015).
 - [37] M. Otsuki and H. Hayakawa, *Physical Review E* **90**, 042202 (2014).
 - [38] C. Coulais, A. Seguin, and O. Dauchot, *Physical Review Letters* **113**, 198001 (2014).
 - [39] C. Rainone, P. Urbani, H. Yoshino, and F. Zamponi, *Phys. Rev. Lett.* **114**, 015701 (2015).
 - [40] L. Berthier, P. Charbonneau, Y. Jin, G. Parisi, B. Seoane, and F. Zamponi, *arXiv:1511.04201* (2015).
 - [41] G.-J. Gao, J. Blawdziewicz, C. S. O’Hern, and M. Shattuck, *Phys. Rev. E* **80**, 061304 (2009).
 - [42] S. Torquato and F. H. Stillinger, *Rev. Mod. Phys.* **82**, 2633 (2010).
 - [43] T. Bertrand, R. P. Behringer, B. Chakraborty, C. S. O’Hern, and M. D. Shattuck, *Phys. Rev. E* **93**, 012901 (2016).
 - [44] T. Maimbourg, J. Kurchan, and F. Zamponi, *Phys. Rev. Lett.* **116**, 015902 (2016).
 - [45] P. Charbonneau, A. Ikeda, G. Parisi, and F. Zamponi, *Phys. Rev. Lett.* **107**, 185702 (2011).
 - [46] A. K. Dubey, I. Procaccia, C. A. Shor, and M. Singh, *arXiv:1512.03244* (2015).
 - [47] P. Sollich, F. Lequeux, P. Hébraud, and M. E. Cates, *Physical review letters* **78**, 2020 (1997).

- [48] L. Balents, J.-P. Bouchaud, and M. Mézard, Journal de Physique I **6**, 1007 (1996).
- [49] G. Biroli and P. Urbani, [arXiv:1601.06724](#) (2016).